New Journal of Physics
The open access journal at the forefront of physics

Deutsche Physikalische Gesellschaft DPG IOP Institute of Physics

PAPER • OPEN ACCESS

Driving protocol for a Floquet topological phase without static counterpart

To cite this article: A Quelle *et al* 2017 *New J. Phys.* **19** 113010

New Journal of Physics
The open access journal at the forefront of physics

Deutsche Physikalische Gesellschaft DPG
IOP Institute of Physics

Published in partnership with: Deutsche Physikalische Gesellschaft and the Institute of Physics

CrossMark

OPEN ACCESS

RECEIVED
2 April 2017

REVISED
3 August 2017

ACCEPTED FOR PUBLICATION
15 August 2017

PUBLISHED
8 November 2017

PAPER

Driving protocol for a Floquet topological phase without static counterpart

A Quelle[1], C Weitenberg[2], K Sengstock[2] and C Morais Smith[1,3]

[1] Institute for Theoretical Physics, Center for Extreme Matter and Emergent Phenomena, Utrecht University, Princetonplein 5, 3584 CC Utrecht, The Netherlands
[2] Institut für Laserphysik, Universität Hamburg, Luruper Chaussee 149, D-22761 Hamburg, Germany
[3] Author to whom any correspondence should be addressed.

E-mail: c.demoraissmith@gmail.com

Keywords: Floquet topological insulator, ultracold atoms, driven systems

Abstract

Periodically driven systems play a prominent role in optical lattices. In these ultracold atomic systems, driving is used to create a variety of interesting behaviours, of which an important example is provided by topological states of matter. Such Floquet topological phases have a richer classification than their equilibrium counterparts. Although there exist analogues of the equilibrium topological phases that are characterised by a Chern number, the corresponding Hall conductivity, and protected edge states, there is an additional possibility. This is a phase that has a vanishing Chern number and no Hall conductivity, but nevertheless hosts anomalous topological edge states (Rudner *et al* (2013 *Phys. Rev.* X **3** 031005)). Due to experimental difficulties associated with the observation of such a phase, it has not been experimentally realised in optical lattices so far. In this paper, we show that optical lattices prove to be a good candidate for its realisation and observation, because they can be driven in a controlled manner. Specifically, we present a simple shaking protocol that serves to realise this special Floquet phase, discuss the specific properties that it has, and propose a method to experimentally detect this fascinating topological phase that has no counterpart in equilibrium systems.

1. Introduction

The field of optical lattices is a flourishing part of modern physics (Bloch *et al* 2008). This is to a large extent due to the extreme tunability of ultracold atomic systems, which allows for the quantum simulation of many paradigmatic models in condensed matter. Since the experimental realisation of topological phases in condensed-matter systems (König *et al* 2007, Hasan and Kane 2010, Qi and Zhang 2010), there has been an intense activity to reproduce and manipulate such states in optical lattices (Goldman *et al* 2016). Important examples are the realization of lattices with artificial gauge fields (Struck *et al* 2012, Aidelsburger *et al* 2013, 2015) and of topological band structures (Wu *et al* 2016).

One possible way to implement the artificial gauge fields required to create such a system is by using Raman-assisted tunnelling (Jaksch and Zoller 2003, Aidelsburger *et al* 2011, Miyake *et al* 2013, Mancini *et al* 2015, Stuhl *et al* 2015), while an alternative is to shake the lattice periodically (Eckardt *et al* 2005, Lignier *et al* 2007, Struck *et al* 2011, Parker *et al* 2013, Jotzu *et al* 2014, Fläschner *et al* 2016). The effective stroboscopic Hamiltonian for such a periodically driven system is obtained using Floquet theory. In the high-frequency regime, the dynamics of the system can be described in terms of an effective static theory. However, due to the non-equilibrium nature of Floquet systems, a much richer behaviour is possible outside of the high-frequency regime (Lindner *et al* 2011, Ezawa 2013, Fregoso *et al* 2013, Wang *et al* 2013, Carpentier *et al* 2015, Quelle and Morais Smith 2014, Kundu *et al* 2014, Quelle *et al* 2016), and their topological classification is more complicated than that of equilibrium systems (Nathan and Rudner 2015): there is a state where all Chern numbers vanish, which is yet topologically non-trivial (Kitagawa *et al* 2010, Rudner *et al* 2013, Reichl and Mueller 2014, Titum *et al* 2016). Because of the non-trivial topology, these systems host protected chiral edge modes, but there is no transverse conductivity in

the bulk, due to the vanishing Chern number. As a consequence, the bulk is no longer robust against Anderson localisation, and it is possible to fully localise the bulk states while preserving the edge states (Titum *et al* 2016). This behaviour is well understood from a theoretical viewpoint, and various models exhibiting these features have been studied (Kitagawa *et al* 2010, Rudner *et al* 2013, Reichl and Mueller 2014, Titum *et al* 2016). Additionally, there is experimental evidence for these states in photonic waveguides (Maczewsky *et al* 2017, Mukherjee *et al* 2017). However, this state has not yet been experimentally realised in optical lattices. Such a realisation is desirable, because optical lattices allow for larger system size, as well as a greater tunability of the internal atomic states and interactions. The ability to tune the hopping strength is of special interest, because it is necessary for the full localisation of the bulk, but the possibility to include interactions is also promising in light of prospective future developments.

In this paper, we propose a simple shaking protocol for a honeycomb optical lattice loaded with fermions that allows for the realisation of this exotic topological state, which bears no analogue in equilibrium systems. We construct the full topological phase diagram for the model, and determine which specific experimental parameters might be used to access the non-trivial phase with vanishing Chern number. Because the Hall conductivity vanishes, the topological nature of this system must be determined by measuring the edge states directly, or by constructing the relevant topological invariant, which requires full tomography of the driving cycle. We show that a 2D honeycomb optical lattice for fermions has favourable properties for measuring the edge states directly.

The layout of the paper is as follows. First, we review the relevant results about Floquet topological insulators (FTIs) in section 2. More specifically, we discuss the topological classification of this system, which is necessary to construct the phase diagram. Then, we determine the time-dependent Hamiltonian corresponding to our shaking protocol in section 3. In section 4, we construct the phase diagram for the model, and provide the dispersion relation at characteristic values of the parameters, as well as an analysis of the robustness of the phase. Then, in section 5, we discuss the conditions for an experimental observation of such a phase in optical lattices. Finally, we conclude in section 6.

2. Floquet topological insulators

Floquet theory applies to time-periodic Hamiltonians (Sambe 1973, Hemmerich 2010), for which the time-dependent Schrödinger equation has quasi-periodic solutions $\psi(t) = \exp(-i\epsilon t/\hbar)\phi(t)$, where ϕ is a periodic function in time and thus a solution of $H_F\phi(0) = \epsilon\phi(0)$. Here, the Floquet Hamiltonian is defined as

$$H_F := -i\ln[U]/T, \tag{1}$$

where $U := U(T, 0)$ is the propagator from $t = 0$ to $t = T$, i.e. over a single period. If H_F exhibits topologically protected edge states for a finite system, one speaks of an FTI. The propagator U is unitary, so its spectrum lies on the unit circle in the complex plane. Because the logarithm maps the unit circle onto the real line, H_F has real spectrum and is Hermitian. If one chooses the branch cut of the logarithm to lie in one of the band gaps of U, H_F will have a top and a bottom energy band. However, if the gap containing the branch cut also contains gapless edge modes, these modes will connect the top and bottom bands of H_F through the branch cut (Rudner *et al* 2013). The full classification of an FTI, taking this effect into account, can be done in terms of winding numbers (Rudner *et al* 2013), Weyl cones (Nathan and Rudner 2015), or by considering the scattering matrix of the system (Fulga and Maksymenko 2016). The classification in terms of winding numbers is more closely analogous to the classification of equilibrium systems in terms of Chern numbers, so we recall it here.

An n-band Floquet system has n gaps Δ_i, where Δ_i is the gap above band i. Note that due to the branch cut in H_F, $\Delta_0 = \Delta_n$. One can associate the winding number W_i to the gap Δ_i (Rudner *et al* 2013). To construct W_i, note that the propagator is periodic in $\boldsymbol{k}$, but not necessarily in t, since $U = U(T, 0) \neq 1$ in general. First, we construct a periodic unitary operator by defining

$$V_i(\boldsymbol{k}, t) = \begin{cases} U(\boldsymbol{k}, 2t) & 0 \leqslant t \leqslant \frac{T}{2} \\ \exp(-i(2T - 2t)H_F) & \frac{T}{2} \leqslant t \leqslant T\,. \end{cases} \tag{2}$$

This equation depends on a choice, since the eigenvalues of U lie on the unit circle. One therefore has to choose a Brillouin zone for the quasi-energies of H_F. Mathematically, this corresponds to a choice of branch cut for the logarithm in equation (1). This means that V_i is only a continuous function of $\boldsymbol{k}$ and t if one chooses the ends of this Brillouin zone to lie in one of the band gaps Δ_i of U. In equation (2) we have assumed that these ends lie in the specific gap Δ_i, and we indicate this through the subscript of V_i. The operator V_i is periodic over the generalised Brillouin zone including time. Hence, we can define the winding number

$$W_i := \frac{1}{8\pi^2}\int_{\mathrm{GBZ}} \mathrm{d}t\mathrm{d}k_x\mathrm{d}k_y\,\mathrm{Tr}\,(V_i^{-1}\partial_t V_i[V_i^{-1}\partial_{k_x}V_i,\ V_i^{-1}\partial_{k_y}V_i,]). \tag{3}$$

Because this integral is a topological winding number, and V_i was defined to be continuous, it is quantised. As can be seen from equation (3), the winding number is also derived from the bulk states, but in contrast to the Chern number, it depends on the full time-evolution operator of the Floquet system, not only on its value at stroboscopic times. It can be shown that W_i equals a sum over all chiral edge modes crossing Δ_i, weighted with a $\pm$, depending on their propagation direction. The Chern number of band i can be expressed as $C_i = W_i - W_{i-1}$, which yields the connection with the Chern number of the bands. In a static system, $W_n = W_0 = 0$, because the spectrum has no branch cut, but is bounded both below and above. This constraint allows one to express the W_i in terms of C_i uniquely. For a Floquet system, W_0 is non-zero when a chiral edge mode crosses the branch cut, and all Chern numbers vanish for a state with $W_i = c$ for all i, while it is topologically non-trivial if the integer c is non-zero. In this case, it is the driving cycle that protects the edge modes, instead of the topology of the bands as for conventional static systems. These trivial bands are not protected from Anderson localisation by topology, which allows for chiral edge modes in combination with a fully localised bulk (Titum *et al* 2016).

3. The model

It is known that a phase with $W_i = 1$ can be created through periodic modulation of nearest-neighbour (NN) hopping parameters either in a bipartite square (Rudner *et al* 2013, Reichl and Mueller 2014) or in a hexagonal lattice (Kitagawa *et al* 2010). In optical lattices, the hopping amplitudes in the different directions can be simply tuned by varying the intensities of the lattice beams (Zhu *et al* 2007). However, we propose here a different approach using lattice shaking (Koghee *et al* 2012), which has clear experimental advantages. First, the hopping amplitudes can be modulated more effectively, allowing for a full suppression of the undesired hopping amplitudes instead of just a finite anisotropy, thus realizing the model considered in (Kitagawa *et al* 2010). Second, the use of lattice shaking might allow for a cleaner implementation of the step-function-like switching of the hopping amplitudes that is at the origin of the perfectly flat bands we discuss later. Thirdly, lattice shaking couples differently to the higher bands than amplitude modulation of the lattice beams, and therefore potentially leads to a smaller heating rate.

The driving protocol takes advantage of the fact that linear shaking of a lattice renormalises the hopping according to the projection of the shaking amplitude onto the bond (Struck *et al* 2011, Koghee *et al* 2012). Specifically, let the lattice be subjected to a sinusoidal shaking

$$\boldsymbol{F}(t) = \sin(\omega t)\boldsymbol{f},$$

where ω is the shaking frequency, and $\boldsymbol{f}$ a vector determining the shaking direction and amplitude, as depicted in figure 1. Then, the NN hopping parameters γ in a tight-binding model become renormalised as

$$\gamma \mapsto \gamma_r = \gamma J_0\left(\frac{m\omega\boldsymbol{d}\cdot\boldsymbol{f}}{\hbar}\right). \tag{4}$$

Here, $\boldsymbol{d}$ is a vector in the bond direction with magnitude equal to the bond length, m is the particle mass, and J_0 is a Bessel function of the first kind. For future reference, let us now define x_0 to be the first zero of J_0. The expression in equation (4) is the first order in a perturbation expansion in terms of the number of exchanged quanta of the driving field and their frequency (Eckardt 2017). Taking this into account, we start from the NN hopping Hamiltonian for a honeycomb lattice:

$$H(\boldsymbol{k}) = \gamma\sum_l\begin{pmatrix} 0 & \exp(\mathrm{i}\boldsymbol{k}\cdot\boldsymbol{d}_l) \\ \exp(-\mathrm{i}\boldsymbol{k}\cdot\boldsymbol{d}_l) & 0\end{pmatrix}. \tag{5}$$

Our convention for the NN hopping vectors $\boldsymbol{d}_l$ is $\boldsymbol{d}_1 = a(0,\ 1)$, $\boldsymbol{d}_2 = a(-\sqrt{3},\ 1)/2$, and $\boldsymbol{d}_3 = -a(\sqrt{3},\ 1)/2$, where a is the NN distance. By shaking in the 2D plane, perpendicularly to a particular bond, $\boldsymbol{d}\cdot\boldsymbol{f} = 0$ for that bond, and $af\ \cos(\pi/6)$ for the other two bonds. By choosing f and ω in equation (4) such that

$$mfa\omega\cos(\pi/6)/\hbar = x_0, \tag{6}$$

we can suppress two of the three hopping parameters through shaking, leaving the third one unaffected. In principle, it is also possible to aim for higher zeroes of the Bessel function than x_0, but since x_0 yields the smallest value of f for a given ω, convergence of the perturbation expansion is best when using x_0. This procedure yields the three renormalised Hamiltonians

$$H_l(\boldsymbol{k}) = \gamma\begin{pmatrix} 0 & \exp(\mathrm{i}\boldsymbol{k}\cdot\boldsymbol{d}_l) \\ \exp(-\mathrm{i}\boldsymbol{k}\cdot\boldsymbol{d}_l) & 0\end{pmatrix}.$$

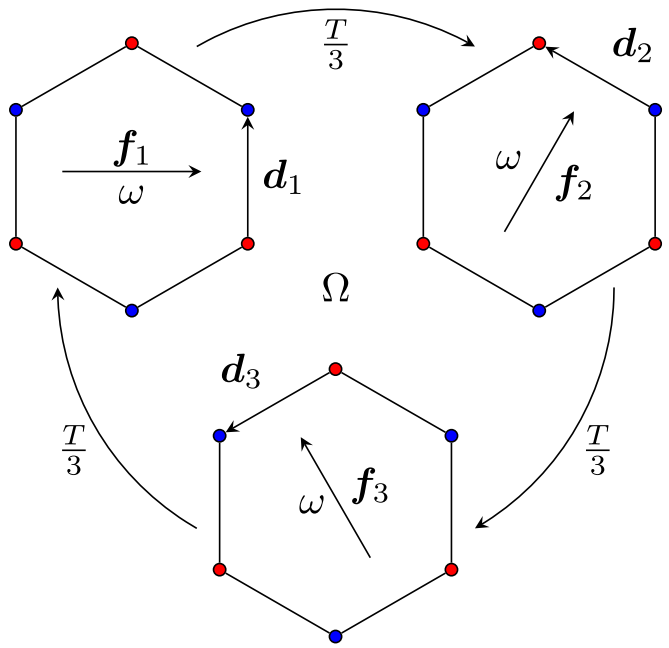

Figure 1. A scheme for the driving protocol is shown. The full driving cycle, with frequency Ω, consists of three separate subcycles, which each last for time $T/3$, a third of the full driving period T. In each of these subcycles, the lattice is shaken in the direction of the vector $\boldsymbol{f}_i$ at frequency ω. The shaking along $\boldsymbol{f}_i$ leaves the hopping parameter along the direction $\boldsymbol{d}_i$ unchanged, and may be chosen such that it renormalises the hopping along the other two directions to zero. The bond vectors d_i are also indicated in the figure, and the net result of the driving is that an atom hops counter-clockwise along the plaquette.

Finally, we consider the system with Floquet propagator

$$U(\boldsymbol{k}) = \prod_l \exp\left[-\frac{\mathrm{i}T}{3\hbar}H_l(\boldsymbol{k})\right], \tag{7}$$

where the product is ordered with higher indices to the left. It should be noted that we apply the Floquet theory two consecutive times, first to construct the effective Hamiltonians H_l, and then to obtain equation (7). Note that we could also have applied Floquet theory only once to the full Hamiltonian with period T and frequency $\Omega := 2\pi/T$. However, by using the intermediate step with the effective Hamiltonians, we are able to derive exact results for the Floquet propagator, such as the phase diagram. We have checked through a numerical calculation of U that the errors induced by this perturbative treatment are negligible if one chooses ω large enough, where the precise meaning of large enough is discussed in section 5. It is, therefore, the full driving frequency Ω that determines the presence of the driving resonances that will lead to the Floquet topological phase. In contrast, ω must be large and obey equation (7) to realise the effective Hamiltonians, which are indeed non-topological. The consecutive application of Floquet theory is only possible if 3ω is a multiple of Ω, since the three individual shaking protocols then fit in the driving cycle in a commensurate way, as depicted in figure 1. The renormalised hopping in equation (4) imposes a constraint on $f\omega$, so by tuning the shaking amplitude f, one can achieve a commensurate ω at any desired value of γ_r.

4. Results

The Floquet propagator in equation (7) can be calculated in closed form as long as translational symmetry is present in the system. To do so, let us write

$$H_l(\boldsymbol{k}) = \gamma[\cos(\boldsymbol{k}\cdot\boldsymbol{d}_l)\sigma_x + \sin(\boldsymbol{k}\cdot\boldsymbol{d}_l)\sigma_y]. \tag{8}$$

We can define partial propagators

$$U_l(\boldsymbol{k}) := \exp\left[-\mathrm{i}\frac{T}{3\hbar}H_l\right] = \cos\left(\frac{\gamma T}{3\hbar}\right) - \frac{\mathrm{i}}{\gamma}\sin\left(\frac{\gamma T}{3\hbar}\right)H_l(\boldsymbol{k}). \tag{9}$$

Here, we have made use of the fact that all the eigenvalues of H_l are $\pm\gamma$, independent of $\boldsymbol{k}$, so that $H_l(\boldsymbol{k})/\gamma$ has unit norm on the Bloch sphere. It follows from the definition that $U = U_3U_2U_1$. To evaluate the various cross-terms in this product, we use

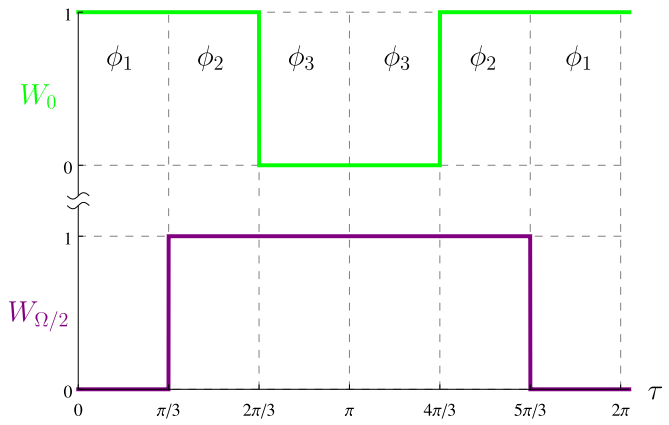

Figure 2. The winding numbers W_0 and $W_{\Omega/2}$ are plotted in green and purple respectively. The different combinations of these two numbers yield three different phases, which are indicated by ϕ_i, for $i = 1, 2, 3$. It should be noted that the gap closes at $\tau = \pi$, so ϕ_3 is not well defined at this point; the gap closing does not change the topological phase, however. The Chern numbers of the bands are given by the difference of the two winding numbers, and therefore take the values 0 and ± 1.

$$\frac{1}{\gamma^2} H_m(\boldsymbol{k}) H_n(\boldsymbol{k}) = \cos[\boldsymbol{k}\cdot(\boldsymbol{d}_m - \boldsymbol{d}_n)] + i\sin[\boldsymbol{k}\cdot(\boldsymbol{d}_m - \boldsymbol{d}_n)]\sigma_z, \qquad \frac{1}{\gamma^3} H_3(\boldsymbol{k}) H_2(\boldsymbol{k}) H_1(\boldsymbol{k}) = \sigma_x.$$

The last equality follows because in our convention $\boldsymbol{d}_1 + \boldsymbol{d}_3 = \boldsymbol{d}_2$, which simplifies the product. This allows us to write

$$\begin{aligned} U(\boldsymbol{k}) = {} & 1[\cos^3(\tau) - \cos(\tau)\sin^2(\tau) \\ & \times \{\cos[\boldsymbol{k}\cdot(\boldsymbol{d}_1 - \boldsymbol{d}_2)] + \cos[\boldsymbol{k}\cdot(\boldsymbol{d}_1 - \boldsymbol{d}_3)] + \cos[\boldsymbol{k}\cdot(\boldsymbol{d}_2 - \boldsymbol{d}_3)]\}] \\ & + \mathrm{i}\sigma_x\{\sin^3(\tau) - \cos^2(\tau)\sin(\tau)[\cos(\boldsymbol{k}\cdot\boldsymbol{d}_1) + \cos(\boldsymbol{k}\cdot\boldsymbol{d}_2) + \cos(\boldsymbol{k}\cdot\boldsymbol{d}_3)]\} \\ & - \mathrm{i}\sigma_y\cos^2(\tau)\sin(\tau)[\sin(\boldsymbol{k}\cdot\boldsymbol{d}_1) + \sin(\boldsymbol{k}\cdot\boldsymbol{d}_2) + \sin(\boldsymbol{k}\cdot\boldsymbol{d}_3)] - \mathrm{i}\sigma_z[\cos(\tau)\sin^2(\tau) \\ & \times \{\sin[\boldsymbol{k}\cdot(\boldsymbol{d}_1 - \boldsymbol{d}_2)] + \sin[\boldsymbol{k}\cdot(\boldsymbol{d}_1 - \boldsymbol{d}_3)] + \sin[\boldsymbol{k}\cdot(\boldsymbol{d}_2 - \boldsymbol{d}_3)]\}]. \end{aligned} \tag{10}$$

Here, $\tau = T\gamma/3\hbar$ is a dimensionless parameter characterising the driving frequency, which is equivalent to specifying Ω in units of γ. The full topological phase diagram can only be obtained by considering the driving cycle leading to this operator through equation (3). However, some information can already be gleaned from equation (10). For example, sending $\tau \mapsto \tau + \pi$ maps $U \mapsto -U$, and consequently $H_F \mapsto H_F + \omega/2$. This shows that the bands are exchanged under this transformation, and so are their Chern numbers. The method above can also be used to calculate $U(t, 0)$, from which one can determine W_0 and $W_{\Omega/2}$ to construct the phase diagram. Here, we have used that $U(t, 0)$ has two energy bands, and that the two corresponding gaps lie at $\epsilon = 0$ and $\epsilon = \Omega/2$ by the symmetry of the Hamiltonian in equation (5). Because of this, one can label the gaps as Δ_0 and $\Delta_{\Omega/2}$, and similarly for the corresponding winding numbers. This phase diagram is 2π periodic in τ, and the first period is depicted in figure 2. Three phases are visible, all of which are topological due to the presence of a gapless edge mode in at least one gap. In the following, we discuss these phases ϕ_i, $i = 1, 2, 3$. Representative dispersions from these phases are plotted in figures 3(a)–(c), respectively, for a ribbon geometry with zigzag edges.

In figure 3(a), we have plotted the dispersion of H_F, as defined using equations (1) and 7, for the parameter value $\tau = 6\pi/25$. The spectrum is shown for two periods of the quasi-energy, to illustrate that $W_0 = 1$ (as evidenced by the chiral edge mode), while $W_{\Omega/2} = 0$. Consequently, this phase also has non-vanishing Chern number. By increasing the frequency, the gap around $\Omega/2$ increases in size (because the period of the spectrum increases, but the bandwidth does not), and one reaches a high-frequency regime in which the system is well described by a static Hamiltonian. The phase of this effective static Hamiltonian, with a single edge state between the two bands, is the topological phase of the Haldane model (Haldane 1988, Quelle *et al* 2016).

A situation that is only possible for Floquet systems occurs when one increases τ, i.e. if one lowers the frequency. When the frequency becomes low enough, the energy bands from different periods of the quasi-energy start to overlap, a situation that physically corresponds to the appearance of resonances due to the driving (Quelle *et al* 2016). In this case, one enters the phase ϕ_2, where these driving resonances also cause topological edge states to appear in the gap around $\Omega/2$, as depicted in figure 3(b).

The distinguishing feature of phase ϕ_2 is that $W_0 = W_{\Omega/2} = 1$, meaning that the Chern numbers of both bulk bands vanish, while each gap hosts an edge mode. For the specific value of $\tau = \pi/2$ used in figure 3(b), the bulk bands of the system are also dispersionless—an interesting feature, since the flat bands together with vanishing Chern number imply that a localised electron state remains localised under time evolution. Note that

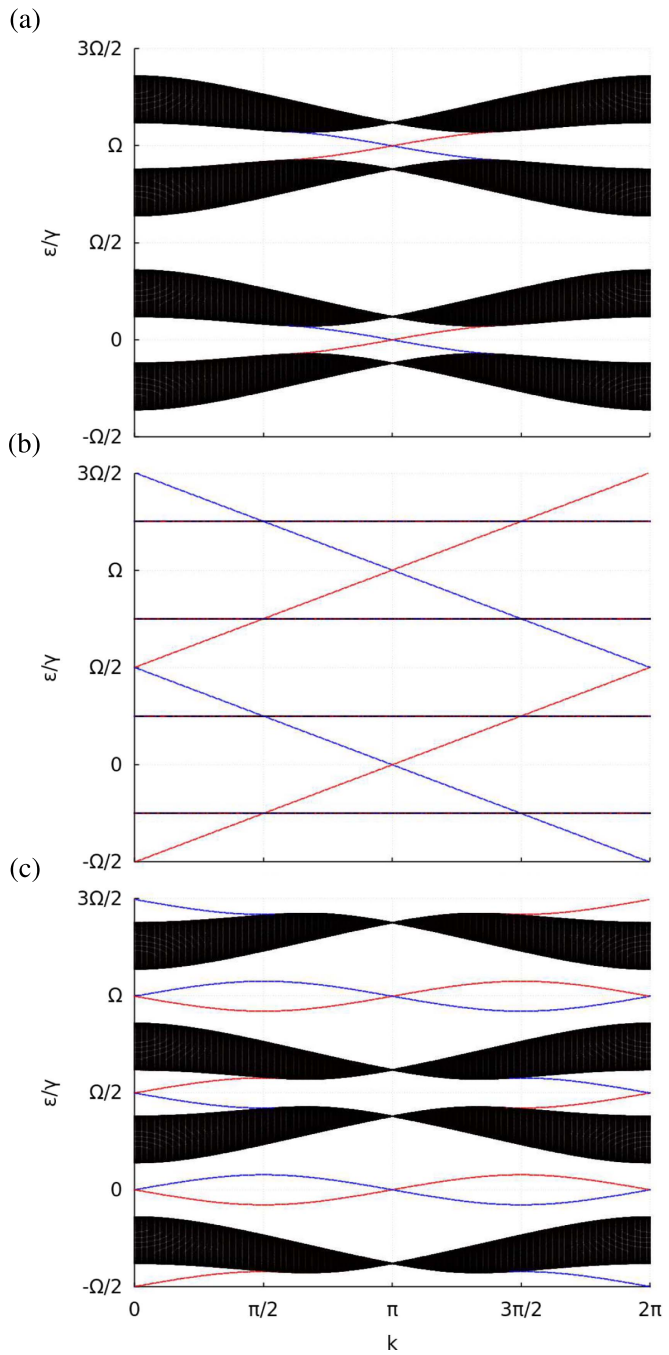

Figure 3. The dispersion of the propagator in equation (7) is shown for a ribbon geometry with zigzag edges for three different values of the driving parameter τ. In all cases there are two energy bands indicated in black, separated by gaps Δ_0 and $\Delta_{\Omega/2}$. The blue and red states are localised on the top and bottom edges, respectively. (a) The parameter $\tau = 6\pi/25$, so the system is in phase ϕ_1. For smaller τ, i.e. larger Ω, the dispersion looks similar, but the gap around $\Omega/2$ becomes larger, so the system behaves more like a static one. (b) The parameter $\tau = \pi/2$, so the system is in phase ϕ_2. By tuning the frequency away from this point, the bulk bands will no longer be flat, but the topological behaviour will be the same. (c) The parameter $\tau = 19\pi/25$, so the system is in phase ϕ_3. The dispersion is like a flipped version of that in (a), where the two gaps have been interchanged. The only difference is the presence of trivial edge states in Δ_0.

in this case, the localisation is not due to Anderson localisation, but due to the driving protocol, making it a different situation from that in (Titum *et al* 2016). The non-zero winding numbers associated with the gap are induced by the chiral nature of the driving protocol, and are thus topological. Consequently, this state can only occur in Floquet systems.

The final phase ϕ_3 is obtained by increasing τ further. The appearance of a two-photon resonance in the system destroys the topological protection of the edge state in Δ_0, as can be seen in figure 2, which shows that $W_{\Omega/2} = 1$, while $W_0 = 0$. A respresentative dispersion relation is shown in figure 3(c). The winding numbers for ϕ_3 imply that the edge state in Δ_0 is not protected by topology, which is consistent with the fact that it is not chiral.

Being topological, these phases should be robust against various kinds of disorder. Due to our intended application in optical lattices, which are inherently defect free, we omit a detailed discussion of the influence of disorder. It is expected that lattice disorder will not destroy the topological phase if the disorder is small enough compared to the gap size. Of greater interest is the robustness of the phase to the parameters that depend on the driving protocol: the Floquet propagator in equation (7) is built from effective Floquet Hamiltonians in which only one of the NN hopping parameters in the honeycomb lattice is assumed to be non-zero. In general, this will not be precisely true, and one of the hopping parameters will merely be much larger than the others. There are two possibilities: the larger hopping parameter may have the same sign as the two smaller ones, or the opposite sign. In both cases, the qualitative behaviour is the same, as we describe in the following. Firstly, it should be noted that the driving frequencies at which the winding numbers W_i change will differ slightly from those depicted in figure 2. Nevertheless, the phase ϕ_2 from figure 3(b) persists even if the smaller hopping parameters become as large as $\gamma/10$, if one is at the point $\tau = \pi/2$. The larger τ becomes, the larger are the deviations from the ideal case presented in equation (7), so the allowed uncertainty in the hopping parameters depends on the value of τ that one intends to work with.

A similar discussion can be held with respect to the presence of next-nearest-neighbour (NNN) hopping. Since NNN hopping naturally occurs in honeycomb optical lattices, a treatment of its effects is important to connect with experiments. In the honeycomb lattice, there are six NNN hopping vectors. These have length $\sqrt{3}\,a$, where a is the NN bond length, as defined previously. Two of these are perpendicular to $\boldsymbol{d}_1$, two to $\boldsymbol{d}_2$, and two to d_3. When shaking according to the protocol discussed above, four of the NNN hopping parameters get renormalised to zero, and the two parallel to the shaking pick up a factor $J_0(2x_0) \approx -0.24$. Hence, the shaking protocol has the added benefit of strongly suppressing the NNN hopping contribution. Now, the phase ϕ_2 is accessible when the *renormalised* NNN hopping parameter is smaller than approximately $\gamma/4$. The *bare* NNN hopping strength depends on the lattice depth, and we will consider below a value of $4\gamma/100$ (Ibañez Azpiroz *et al* 2013). This is clearly within the required range, so NNN hopping will not influence the experimental realisability of this phase. It must be noted that in the presence of NNN hopping the bulk bands are no longer completely flat, but the topological characteristics of the phase remain unchanged.

5. Experimental realisation

It should, therefore, be possible to tune the hopping parameters in such a way that the phase ϕ_2, which is characterised by a non-trivial topological structure but vanishing Chern numbers, can be reached. In light of this fact, we will now discuss some possible experimental parameters that might allow the experimental realisation of the phase ϕ_2 in optical lattices.

The condition that the renormalised hopping parameters in equation (4) vanish imposes a constraint on the shaking amplitude and frequency: $J_0(m\,f\;a\;\omega\cos(\pi/6)/\hbar) = 0$. Assuming that one uses the first solution to this equation, one can rewrite it in terms of the recoil energy $\hbar\pi^2/2\;ma^2$ as

$$\frac{\omega}{\omega_{\mathrm{rec}}} = \frac{4x_0}{\sqrt{3}\,\pi^2}\frac{a}{f}. \tag{11}$$

The recoil energy depends on the particle mass and on the lattice constant, and it is the only parameter in equation (11) that depends on the atomic species loaded into the lattice. For the realisation of the phase ϕ_2, taking $\tau = \pi/2 \bmod \pi$ is preferable. As shown in figure 3(b), the bands are flattest for this value, which is desirable for the reasons that we discuss below. The highest total frequency for which this holds is $\hbar\Omega = 4\gamma/3$. That Ω is constrained by a maximal value shows that it has to be small enough for resonances in the driving to appear, which is a necessity for the realisation of the phase ϕ_2. From now on, we will assume that $\hbar\Omega$ takes this maximal value, since it corresponds to the shortest time scale for the experiment. Since the two shaking frequencies have to be commensurate, $\omega = 3n\Omega$ for $n \in \mathbb{N}$, which corresponds to a shaking amplitude f given by equation (11). Because of equation (11), increasing n requires a lowering of f, but since both parameters can be tuned within a wide range, many possible values can be chosen. For concreteness, we will assume $n = 2$, which corresponds to $\hbar\omega = 8\gamma$. By numerically solving the Schrödinger equation for the full propagator, we have verified that the corresponding values of ω and f are such that the model discussed in section 4 is accurate. In contrast, choosing $n = 1$ (corresponding to $\hbar\omega = 4\gamma$) would result in notable deviations from the effective model. This gives precise meaning to the claim that the effective model works well if ω is large enough. The NN hopping of fermions in an optical lattice is usually expressed in terms of ω_{rec}, since it naturally incorporates the effect of particle mass and the lattice constant. We consider a lattice depth of $7\omega_{rec}$, which corresponds to $\gamma = \hbar\omega_{rec}/10$, and a NNN hopping of $4\omega_{rec}/1000$ (Ibañez Azpiroz *et al* 2013). Using these values for the hopping parameters, and combining these with the chosen value of τ, we find the driving frequency of the system to be $\Omega \approx 4\omega_{rec}/30$, which is about $0.13\omega_{rec}$.

We can obtain specific numbers by choosing a particle mass and an optical wavelength, which allows us to specify a and ω_{rec}. Let us consider fermionic ^{40}K loaded in a honeycomb optical lattice with wavelength $\lambda = 1064$ nm, which amounts to a recoil frequency $\omega_{rec}/2\pi = 4.41$ kHz, and consequently, the minimal driving period $T = 1.7$ ms. The minimal commensurate shaking frequency ω is then $0.4\omega_{rec}/2\pi \approx 1.76$ kHz, which corresponds to a maximal shaking amplitude of $0.075a$. Since the lattice constant is $2\lambda/3$ for a honeycomb lattice, the maximum shaking amplitude $f \approx 53$ nm.

As mentioned earlier, the same phase can be obtained for a variety of parameters. For instance, the frequency ω can be chosen to be any multiple of $0.4\omega_{rec}$, as might be desired to minimise coupling to other bands in the lattice. The shaking amplitude will then be the corresponding fraction of 53 nm. Furthermore, due to the periodicity of the phase diagram, the phase ϕ_2 can also be realised most generally if $(2n + 1)\hbar\Omega = 4\gamma/3$. Choosing $n > 0$ allows one to use a lower Ω, and a correspondingly lower ω.

The distinguishing feature of the phase ϕ_2 is the presence of edge states, while there is neither time-reversal symmetry, nor a non-vanishing Chern number. The Chern number can be measured in terms of the Hall conductivity, which has been achieved in optical lattices (Aidelsburger *et al* 2015), so one can experimentally prove that the Chern number vanishes in this topological phase. There are, nevertheless, edge modes present in the system, protected by the topological nature of the winding numbers associated with the quasi-energy gaps in the system.

The contribution to the transverse conductivity from a fully filled band is given by its Chern number. The fact that the phase ϕ_2 is dynamic in origin does not alter this conclusion. The total wavefunction corresponding to a single occupied energy band of the Floquet propagator is time dependent, returning to itself only after each period T, but this time evolution is unitary. The Chern number, because it is a topological invariant, is invariant under unitary transformations, so the Hall conductivity is constantly zero.

It is, therefore, necessary to detect the topological phase in a different way. One alternative would be to directly detect the edge states to prove the presence of a topological phase in the system. The principal difficulty in 2D systems is the presence of dispersive bulk bands, together with the fact that the edge mode is not present for all k. For this reason, an atom inserted at the edge of a system will have an overlap with the bulk modes, since a localised state has equal overlap with all momenta. If the bulk is dispersive, this overlap will cause the atomic wavefunction to partially leak away into the bulk, making a measurement of the edge state difficult at longer timescales. As can be seen in figure 3(b), for certain parameter values the bulk is nearly dispersionless, while the edge states exist for nearly all k values. This makes the currently proposed system conducive to the direct measurement of topological edge states.

To make the behaviour of edge states in this system explicit, we have shown the time evolution of one such state in figure 4. To make a connection with experiments, we have taken the system discussed in section 4, and included the NNN hopping of $\gamma/10$ that is present in an actual system. Because this term gives the dominant deviation from the phase in figure 3(b), we assume that all other parameters have exactly the right values. To simulate a realistic edge, we have included a potential step of height 10γ, along the line $y = 0$. This cuts the system into two domains separated by zigzag edges along the potential step. Such sharp steps have been realised in quantum gas microscopes (Tai *et al* 2017), and provide a promising approach to the generation of a topological boundary mode experimentally. To show that this indeed leads to well-defined edge states, we have plotted the wavefunction at different times, showing its localisation along the domain wall. The initial state has a constant non-vanishing amplitude for three unit cells along the wall at $y = 1$ and $y = 2$, as shown in figure 4(a). The time evolution indicates that the part of the wavefunction located on the A-sites of the edge (the tips of the zigzag, at $y = 1$) stay localised there with a probability of approximately 90%, while the part of the wavefunction at $y > 1$ slowly disperses into the bulk.

It should be noted that this feature is only topologically protected in the limit of infinite step size, which splits the system into two. For such an infinite step, the system has a protected edge mode on either side of the step, and they counterpropagate (one is the top edge of one system, and the other the bottom edge of the other system). For a finite step size, there will be a small hybridisation between these two states, and the feature is no longer topologically protected. This hybridisation causes some leaking of the wavefunction to the other side of the step, which causes the bidirectional movement that can be seen in figure 4. This bidirectional movement takes place on opposite sides of the potential step, and is suppressed with increasing step size. Nevertheless, if the system were not topological, one would not see the clear propagation along the potential step, but only the diffusive behaviour into the bulk. Note that the dispersion into the bulk is due to the NNN hopping, because at $\tau = \pi/2$ the bulk bands are completely flat in its absence, as shown in figure 3(b). Since the bulk is only weakly dispersive, the edge states have a higher group velocity, and the edge part of the wavefunction clearly separates from the bulk part. This shows that the combination of very flat bulk bands with edge states that exist for most k values ensures that the edge and bulk parts of a wavefunction can be clearly separated from the dynamics.

Instead of detecting the edge state directly, an alternative experimental approach would be to obtain the bulk winding number in equation (3), which dictates the presence of edge states. Recent advances in time-resolved

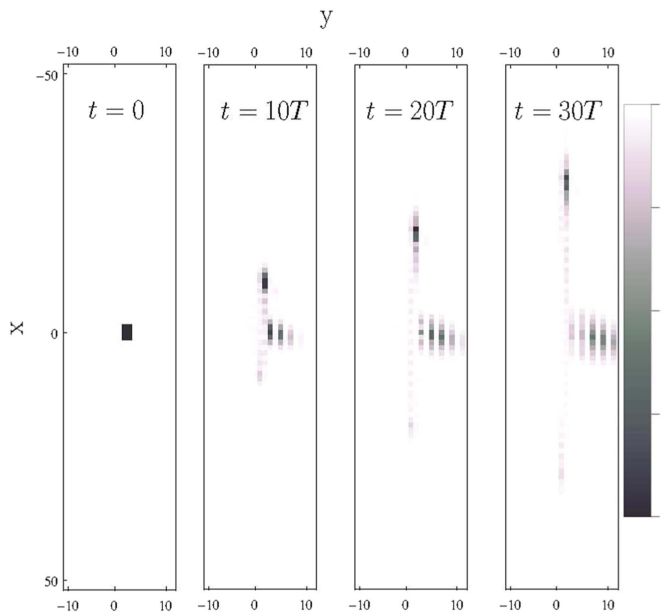

Figure 4. The probability density is depicted at four different times for a system with a sharp potential wall of height 10γ, for $\tau = \pi/2$ and a *bare* NNN hopping of $\gamma/10$, which corresponds to the parameter values discussed in the text. The coordinates x, y label sites of the lattice using the lattice vectors. The lattice vector associated with x lies parallel to the wall, meaning that x is periodic, while the vector associated to y points away from the wall. It should be noted that y is also used to label sublattice, so that $\mathrm{y} = \pm 1$ are the A-sites adjacent to the wall, $\mathrm{y} = \pm 2$ are the B-sites adjacent to the wall, etc. The parameter ranges are $\mathrm{x} \in (-200,\ 200]$ and $\mathrm{y} \in [-100,\ 100]$ (meaning 50 unit cells on either side), but due to the localisation of the wavefunction, only part of the system is shown.

state tomography (Fläschner *et al* 2016, 2016) could allow for a direct measurement of the winding number in equation (3).

6. Conclusion

Floquet systems allow for the realisation of a curious topological phase, which is characterised by vanishing Chern numbers for all bands, while exhibiting topologically protected edge states. Due to the vanishing Chern number, there is no Hall conductivity in the bulk, and the bulk states can localise. This has a surprising consequence for Laughlin's charge pumping argument (Laughlin 1981). Consider, therefore, an infinitely long strip. Since there is no Hall conductivity present in the system, briefly turning on the analogue of a longitudinal electric field (by tilting the lattice, for example), will not pump charge from one edge of the system to the other. In general, turning on such an electric field will cause charge to dissipate into the bulk, but for the situation in figure 3(b) even this does not occur. The periodicity of the Floquet spectrum, together with the perfectly flat bulk bands, is what makes this possible. Take, for example, the red edge state at $k = \pi$ and $\epsilon = 0$. If one adds an infinitesimal longitudinal electric field to the system, this state will move along the red curve towards larger k, and eventually it will reach the red state at $k = 2\pi$ and $\epsilon = \Omega\gamma/2$. Because the spectrum is periodic in both ϵ and k, this state is equivalent to the red state at $k = 0$ and $\epsilon = -\Omega\gamma/2$. After this, the state will continue to move towards larger k, and it will eventually return to $k = \pi$ and $\epsilon = 0$. This shows that applying the analogue of an electric field will merely move charge along the edge, as we have checked through a numerical calculation, and this is possible because the edge spectrum forms a closed loop and the bulk bands are flat. In contrast, starting from the red state at $k = \pi$ and $\epsilon = 0$ in figure 3(a), upon applying the electric field, the edge state will move towards larger k along the red curve until it reaches the bulk states. Because the bulk bands are not flat, the edge mode will move into the bulk, and keep moving towards larger k until it reaches the blue edge states. Since the bulk has non-zero Chern number in this case, the state will also exit the bulk band and move onto the blue line.

Several models that exhibit such a Floquet topological phase have been proposed (Kitagawa *et al* 2010, Rudner *et al* 2013, Reichl and Mueller 2014, Titum *et al* 2016), and an experimental realisation with cold atoms would be desirable. We propose a simple shaking protocol for a honeycomb optical lattice that allows for an experimental realisation of the model in (Kitagawa *et al* 2010), and we discuss possible experimental advantages of this approach. Because Chern numbers have been measured in 2D Floquet optical lattices (Jotzu *et al* 2014, Aidelsburger *et al* 2015, Fläschner *et al* 2016), it is experimentally possible to show the vanishing of the Hall conductivity in this phase. The direct detection of topological edge states in optical lattices remains an

experimental challenge: so far, edge states have only been experimentally observed in 1D systems (Leder *et al* 2016), ladder systems (Atala *et al* 2014, Tai *et al* 2017) or artificial dimensions (Mancini *et al* 2015, Stuhl *et al* 2015). However, promising proposals for their detection in 2D systems exist using either Raman spectroscopy (Goldman *et al* 2012) or the different dynamics of the bulk and edge states after the removal of a barrier (Goldman *et al* 2013). Detection methods involving sharp walls are especially promising for the system under discussion. By tuning the parameters, it is possible to make the bulk bands nearly flat, ensuring that the wavefunction of an atom injected at such a wall has minimal leakage into the bulk.

Beyond the scenario of edges induced by sharp walls, promising prospects include interfaces between regions of different topology induced by spatially varying lattice parameters (Reichl and Mueller 2014, Goldman *et al* 2016). This scenario could apply to our proposal because the phase transitions are controlled by the shaking frequency relative to a resonance that depends on the spatially varying lattice depth.

Alternatively, recent advances in state tomography (Fläschner *et al* 2016a, 2016b) could allow for a direct measurement of the winding number in equation (3). Together, these properties might make the present proposal a promising candidate for the experimental realisation and detection of a Floquet topological phase that has no static counterpart.

Acknowledgments

The work by AQ and CMS is part of the D-ITP consortium, a program of the Netherlands Organisation for Scientific Research (NWO) that is funded by the Dutch Ministry of Education, Culture and Science (OCW). CW and KS acknowledge financial support from the excellence cluster 'The Hamburg Centre for Ultrafast Imaging —Structure, Dynamics and Control of Matter at the Atomic Scale'.

References

Aidelsburger M, Atala M, Lohse M, Barreiro J T, Paredes B and Bloch I 2013 *Phys. Rev. Lett.* **111** 185301
Aidelsburger M, Atala M, Nascimbène S, Trotzky S, Chen Y A and Bloch I 2011 *Phys. Rev. Lett.* **107** 255301
Aidelsburger M, Lohse M, Schweizer C, Atala M, Barreiro J, Nascimbnne S, Cooper N, Bloch I and Goldman N 2015 *Nat. Phys.* **11** 162
Atala M, Aidelsburger M, Lohse M, Barreiro J, Paredes B and Bloch I 2014 *Nat. Phys.* **10** 588–93
Bloch I, Dalibard J and Zwerger W 2008 *Rev. Mod. Phys.* **80** 885–964
Carpentier D, Delplace P, Fruchart M and Gawedzki K 2015 *Phys. Rev. Lett.* **114** 106806
Eckardt A 2017 *Rev. Mod. Phys.* **89** 011004
Eckardt A, Weiss C and Holthaus M 2005 *Phys. Rev. Lett.* **95** 260404
Ezawa M 2013 *Phys. Rev. Lett.* **110** 026603
Fläschner N, Rem B, Tarnowski M, Vogel D, Lühmann D S, Sengstock K and Weitenberg C 2016a *Science* **352** 1091–4
Fläschner N, Vogel D, Tarnowski M, Rem B S, Lühmann D S, Heyl M, Budich J C, Mathey L, Sengstock K and Weitenberg C 2016b (arXiv:1608.05616)
Fregoso B M, Wang Y H, Gedik N and Galitski V 2013 *Phys. Rev.* B **88** 155129
Fulga I C and Maksymenko M 2016 *Phys. Rev.* B **93** 075405
Goldman N, Beugnon J and Gerbier F 2012 *Phys. Rev. Lett.* **108** 255303
Goldman N, Budich J and Zoller P 2016 *Nat. Phys.* **12** 639–45
Goldman N, Dalibard J, Dauphin A, Gerbier F, Lewenstein M, Zoller P and Spielman I B 2013 *Proc. of the Nat. Acad. of Sci.* **110** 6736–41
Goldman N, Jotzu G, Messer M, Görg F, Desbuquois R and Esslinger T 2016 *Phys. Rev.* A **94** 043611
Haldane F 1988 *Phys. Rev. Lett.* **61** 2015–8
Hasan M Z and Kane C L 2010 *Rev. Mod. Phys.* **82** 3045–67
Hemmerich A 2010 *Phys. Rev.* A **81** 063626
Ibañez Azpiroz J, Eiguren A, Bergara A, Pettini G and Modugno M 2013 *Phys. Rev.* A **87** 011602
Jaksch D and Zoller P 2003 *New J. Phys.* **5** 56
Jotzu G, Messer M, Desbuquois R, Lebrat M, Uehlinger T, Greif D and Esslinger T 2014 *Nature* **515** 237
Kitagawa T, Berg E, Rudner M and Demler E 2010 *Phys. Rev.* B **82** 235114
Koghee S, Lim L K, Goerbig M and Morais Smith C 2012 *Phys. Rev.* A **85** 023637
König M, Wiedmann S, Brüne C, Roth A, Buhmann H, Molenkamp L W, Qi X L and Zhang S C 2007 *Science* **318** 766
Kundu A, Fertig H and Seradjeh B 2014 *Phys. Rev. Lett.* **113** 236803
Laughlin R B 1981 *Phys. Rev.* B **23** 5632–3
Leder M, Grossert C, Sitta L, Genske M, Rosch A and Weitz M 2016 *Nat. Commun.* **7** 13112
Lignier H, Sias C, Ciampini D, Singh Y, Zenesini A, Morsch O and Arimondo E 2007 *Phys. Rev. Lett.* **99** 220403
Lindner N, Refael G and Galitski V 2011 *Nat. Phys.* **7** 490–5
Maczewsky L, Zeuner J, Nolte S and Szameit A 2017 *Nat. Comm.* **8** 13756
Mancini M *et al* 2015 *Science* **349** 1510–3
Miyake H, Siviloglou G A, Kennedy C J, Burton W C and Ketterle W 2013 *Phys. Rev. Lett.* **111** 185302
Mukherjee S, Spracklen A, Valiente M, Andersson E, Öhberg P, Goldman N and Thomson R 2017 *Nat. Comm.* **8** 13918
Nathan F and Rudner M S 2015 *New J. Phys.* **17** 125014
Parker C V, Ha L C and Chin C 2013 *Nat. Phys.* **9** 769
Qi X L and Zhang S C 2010 *Phys. Today* **63** 33
Quelle A, Goerbig M O and Morais Smith C 2016 *New J. Phys.* **18** 015006
Quelle A and Morais Smith C 2014 *Phys. Rev.* B **90** 195137

Reichl M D and Mueller E J 2014 *Phys. Rev.* A **89** 063628
Rudner M, Lindner N H, Berg E and Levin M 2013 *Phys. Rev.* X **3** 031005
Sambe H 1973 *Phys. Rev.* A **7** 2203–13
Struck J, Ölschläger C, Targat R L, Soltan-Panahi P, Eckardt A, Lewenstein M, Windpassinger P and Sengstock K 2011 *Science* **333** 996–9
Struck J, Ölschläger C, Weinberg M, Hauke P, Simonet J, Eckardt A, Lewenstein M, Sengstock K and Windpassinger P 2012 *Phys. Rev. Lett.* **108** 225304
Stuhl B, Lu H I, Aycock L, Genkina D and Spielman I 2015 *Science* **349** 1514–8
Tai M E, Lukin A, Rispoli M, Schittko R, Menke T, Borgnia D, Preiss P M, Grusdt F, Kaufman A M and Greiner M 2017 *Nature* **546** 519–23
Titum P, Berg E, Rudner M S, Refael G and Lindner N H 2016 *Phys. Rev.* X **6** 021013
Wang Y, Steinberg H, Jarillo-Herrero P and Gedik N 2013 *Science* **342** 453–7
Wu Z, Zhang L, Xu X T, Wang B Z, Deng S C J Y, Chen S, Liu X J and Pan J W 2016 *Science* **354** 83–8
Zhu S L, Wang B and Duan L M 2007 *Phys. Rev. Lett.* **98** 260402